Benha Journal of Engineering Science and Technology

BJEST (2025) Vol. 2 Issue (1) pp: 25-10
DOI:
https://bjest.journals.ekb.eg/

Aerodynamic Enhancements of the S834 Airfoil for Small-Scale Wind Turbines: Addressing Flow Separation with Slot Modifications

Khaled Y. Elwan [a], Abdelgalil Eltayesh [a], Saeed A. El-Shahat [a], Mahmoud E. Hasan [a], Hesham M. El-Batsh [a,b]

[a] *Mechanical Engineering Department, Benha Faculty of Engineering, Benha University, Egypt.*

[b] *Currently Professor and Dean of Higher Institute of Engineering and Technology at Mahala El-Kobra, Egypt*

khaled.elwan@bhit.bu.edu.eg

Keywords:
S834 airfoil
Horizontal axis wind turbines,
Passive flow control,
Slots.

A B S T R A C T

Renewable energy plays a crucial role in building a sustainable and environmentally friendly future. Among the available sources, wind energy has immense potential to meet increasing global energy demands. However, one of the key aerodynamic challenges faced by wind turbines is flow separation, which affects efficiency. This study employs computational fluid dynamics (CFD) to analyze the unsteady aerodynamic behavior of an S834 wind turbine airfoil. The research focuses on assessing the impact of incorporating a slot as a passive flow control mechanism across a broad range of angles of attack from 2 to 18 and wind speed 6m/d. The findings indicate that the slotted airfoil significantly enhances aerodynamic performance, particularly at moderate to high angles of attack. Compared to the baseline airfoil, the slotted configuration exhibits increased lift and reduced drag, leading to a notable improvement in aerodynamic efficiency. The analysis of streamlines confirms reduced flow separation on the suction side, while the static pressure distribution further supports the findings. These results highlight the effectiveness of slot implementation in improving wind turbine airfoil efficiency and overall aerodynamic stability.

1. Introduction

Airfoils are essential components in the design of aerodynamic surfaces used in various applications, such as aircraft wings, wind turbine blades, and other lifting surfaces. As a result, several technical solutions are being investigated to improve airfoil efficiency, including boosting lift, diminishing drag, and delaying stall angle. The main challenge of the airfoil occurring at a higher angle of attack (AOA) is that the flow may become more adverse and separate from the wing, causing a loss of lift and increased drag, thereby compromising their performance [1].

The S834 airfoil, created by the National Renewable Energy Laboratory (NREL), is one of the family of quiet, thick, natural-laminar-flow airfoils designed and theoretically evaluated for 1-3 meter-diameter, horizontal-axis wind turbines (HAWTs) [2]. Consequently, studies on this airfoil have become critical to improving the aerodynamic properties of small-scale HAWTs. Skaltsogiannis et al. [3] examined the steady-state two-dimensional flow over the S834 airfoil at various angles of attack using Computational Fluid Dynamics (CFD). The simulations were performed at Reynolds numbers of 3.5×10^5 and 5×10^5, with different turbulence models. The study found a relative error increase in the computational results at higher angles of attack. In contrast, perfect results occurred at low attack angles, closely matching the experimental data. In addition, Hasan et al. [2] investigated experimentally and numerically the performance of commercial small-scale HAWT using S834 as part of a commercial small-scale wind turbine. The results pointed to the importance of airflow behavior and flow separation control in increasing the power coefficient

of the wind turbines. These studies indicate challenges in accurately predicting aerodynamic coefficients under these conditions.

To address this issue, scientists have explored various methods [4] [5] [6] to enhance the performance of airfoils at high angles of attack. The current research aims to build upon these studies by explicitly examining the role of a slot in mitigating flow separation and improving the stall resistance of the NACA 834 airfoil. The slot technique is one of the most considerable ones for mitigating flow separation and improving the stall resistance of the NACA 834 airfoil. A slotted S834 airfoil was compared with the baseline airfoil through simulation studies. The comparison was made regarding the lift-to-drag ratio at a Reynolds number of 105.

The objective of this research is to compare numerically the aerodynamic performance of the NACA 834 airfoil in its slotted and non-slotted configurations. The key parameters under investigation include the lift-to-drag ratio with variable angle of attacks. By evaluating these aspects, this paper aims to provide insight into how a slot can improve the overall aerodynamic efficiency of the airfoil. The study will contribute to the growing body of knowledge regarding flow control devices and their potential applications in enhancing the performance of airfoils in various aerodynamic systems.

2. The physical model and Numerical simulation

The present study explores the impact of a slot-based passive flow control strategy on the aerodynamic characteristics of the S834 airfoil. Figure 1 provides visual representations of the baseline S834 airfoil and its slotted variant, respectively. The computational domain, established based on existing literature, is illustrated in Figure 2. To define the flow boundaries, an inlet velocity condition is applied at both the inlet and the far-field, while a pressure outlet condition is specified at the exit. The computational domain extends 25 chord lengths (C) in the streamwise direction and 20C in the transverse direction to ensure accurate flow development and minimize boundary effects. The airfoil itself is modeled as a stationary no-slip wall, preventing relative motion between the airfoil surface and the fluid.

For numerical simulations, ANSYS Fluent 18.1 is utilized, employing the Unsteady Reynolds-Averaged Navier-Stokes (URANS) equations to resolve the transient aerodynamic behavior. The Shear Stress Transport (SST) k-ω turbulence model is adopted due to its well-known accuracy in capturing boundary layer separation and adverse pressure gradients. A coupled solver is implemented to enhance computational efficiency and solution stability.

To ensure reliable simulation outcomes, a grid independence study is conducted for both the baseline and slotted airfoils at a free-stream velocity of 6 m/s and an angle of attack (AoA) of 12 degrees. Three distinct grid resolutions are tested for both airfoil configurations, as detailed in Table 1, to determine an optimal mesh density. The final computational mesh is depicted in Figure 2. After evaluating variations in aerodynamic coefficients, the selected grid comprises approximately 170,000 elements for the baseline airfoil and 201,900 for the slotted airfoil. This refinement ensures that discrepancies in lift coefficient, drag coefficient, and lift-to-drag ratio remain less than 5% threshold, thereby confirming the mesh's adequacy in capturing key aerodynamic phenomena. The resulting aerodynamic coefficients, including lift, drag, and lift-to-drag ratio, were obtained from the following equations:

$$C_l = \frac{L}{0.5\rho C U_\infty^2} \qquad (1)$$

$$C_d = \frac{D}{0.5\rho C U_\infty^2} \qquad (2)$$

L: lift force
D: drag force
C: chord length
ρ: density
U_∞: free stream velocity

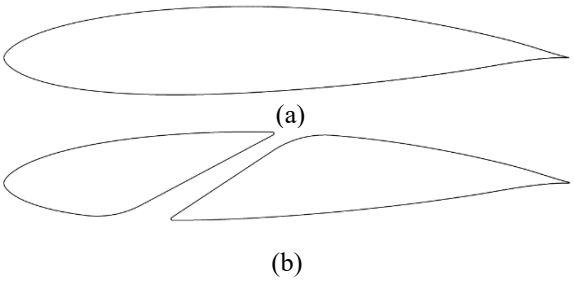

(a)

(b)

Figure 1(a) Unslotted airfoil of 2834 (b) slotted airfoil

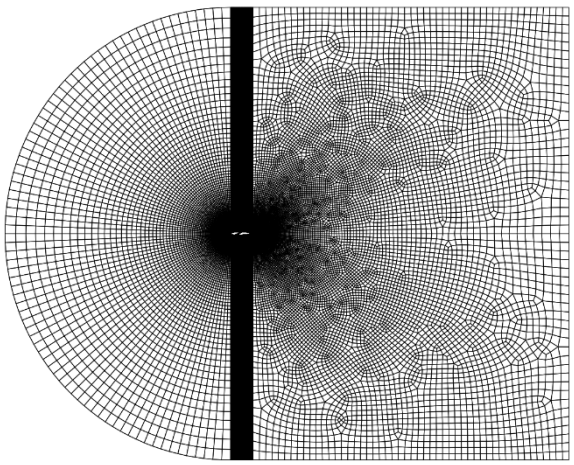

(a)

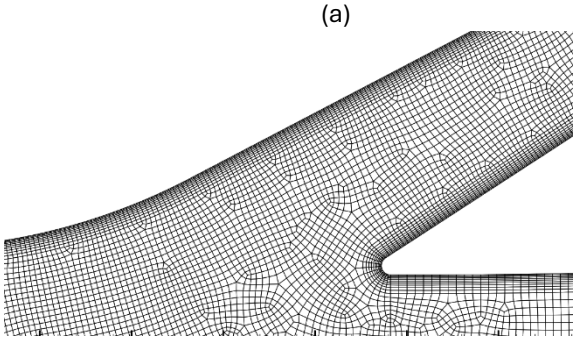

(b)

Figure 2 (a)Flow domain and mesh around airfoil. (b) mesh inside slot

Table 1 mesh independency for unslotted and slotted airfoil.

	No of cells	C_l	C_d	C_l/C_d
Unslotted airfoil	90,000	0.95857	0.05633	17.0165
	170,000	0.97615	0.05384	18.13
	314,000	0.98338	0.053639	18.333
Slotted airfoil	135,350	1.1846	0.0504	23.505
	201,900	1.1853	0.049782	23.809
	266,500	1.1855	0.049615	23.895

3. Results and discussion

The aerodynamic performance of the S834 airfoil was evaluated by comparing the drag coefficient (Cd), lift coefficient (CL), and lift-to-drag ratio (CL/Cd) for both slotted and unslotted configurations across a range of angles of attack (AoA) from 2 to 18. The results are summarized as follows:

The lift coefficient of slotted airfoil exhibits consistently higher values compared to the unslotted configuration across a wide range of angles of attack. The peak lift coefficient for the slotted airfoil is significantly higher by 21% as shown in figure 3.

Drag coefficient at lower angles of attack shows similar behavior in both configurations, with only minimal differences. However, as the AoA increases beyond approximately 10°, the drag coefficient increases more significantly. The unslotted airfoil exhibits slightly higher drag at higher AoA values compared to the slotted configuration, particularly beyond 14°as shown in figure 4.

The slotted airfoil achieves a higher CL/Cd ratio within the moderate AoA range, particularly between 6° and 14°, indicating enhanced aerodynamic efficiency. Additionally, the peak CL/Cd value is greater for the slotted airfoil, demonstrating the beneficial impact of the slot mechanism on overall performance. Beyond 14° AoA, the CL/Cd ratio decreases for both configurations due to rising drag and the onset of stall; however, the slotted airfoil continues to exhibit a slight performance advantage over the unslotted version as shown in figure 5.

The streamlines and velocity contours, shown in Figure 6, which visually support these findings related to the lift, drag, and lift-to-drag coefficients. For wind speed 6m/s, at small angles of attack ranging from 2° to 8°, the suction side of the base airfoil showed no flow separation except small vortex and end corner of the airfoil. Consequently, the slotted airfoil did not provide any performance enhancement; instead, the vortex generated within the slot resulted in a reduction in the lift-to-drag ratio. The slotted airfoil performs best at higher angles of attack, between 10° and 16°, where the slot effectively mitigates the vortex formation at the upper side (suction) of the base airfoil. This improvement is reflected in the enhanced lift-to-drag ratio.

Figures 7 to 11, along with equation 3, demonstrate that at small angles of attack (ranging from 2° to 8°), the static pressure coefficient (Cps) decreases at lower side of original airfoil (pressure side), while increases at the suction side increases. This results in a reduction in the lift-to-drag ratio. Conversely, while for moderate to high angles of attack, the static pressure coefficient at the pressure side increases and decreases at the suction side, leading to an enhancement in the lift-to-drag ratio. These observations are consistent with previously obtained results.

$$\mathrm{Cps} = \frac{p - p_\infty}{0.5\rho C U_\infty^2} \qquad (3)$$

ρ: density

U_∞: free stream velocity

p: static pressure

p_∞: static pressure at the inlet

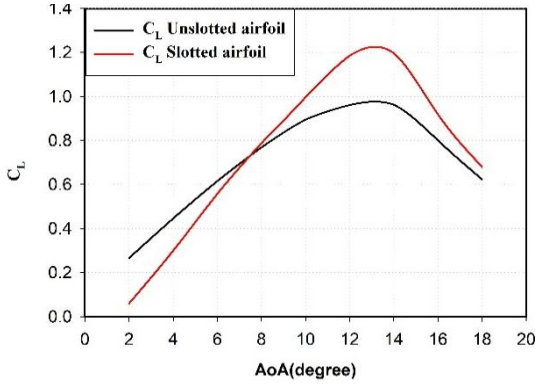

Figure 3 lift coefficient for slotted and unslotted airfoil s834.

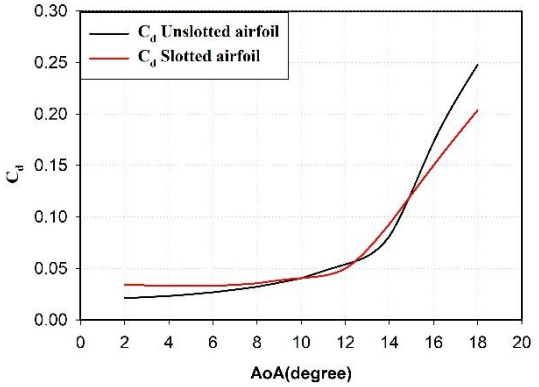

Figure 4 drag coefficient for slotted and unslotted airfoil s834

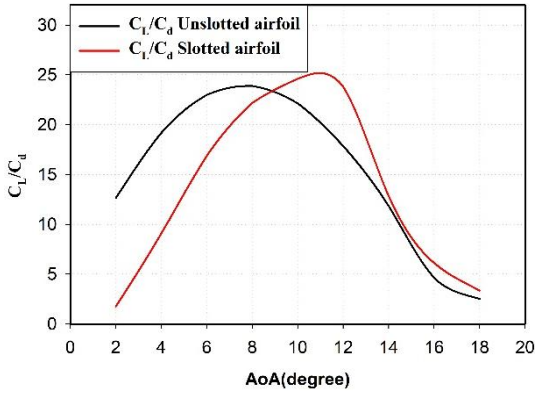

Figure 5 lift to drag coefficient for slotted and unslotted airfoil s834

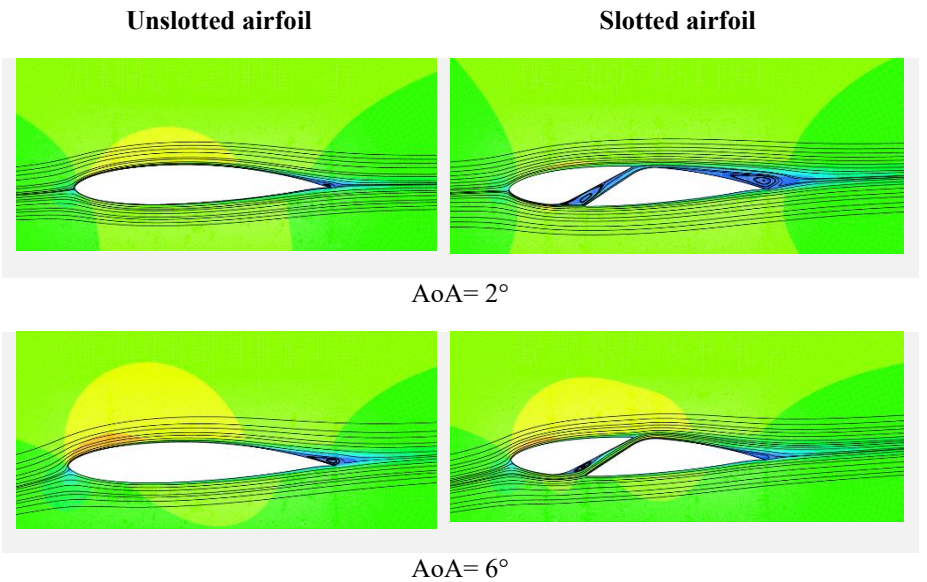

Figure 6 velocity contour and streamlines for slotted and unslotted airfoil.

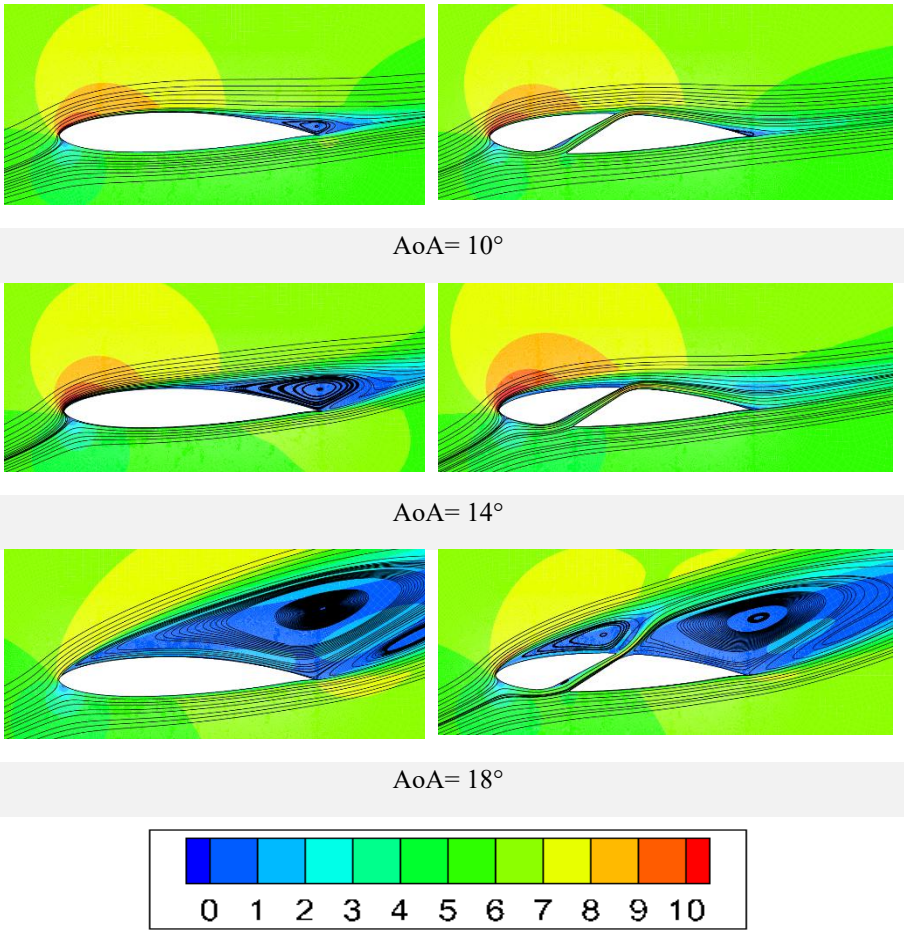

Figure 7 velocity contour and streamlines for slotted and unslotted airfoil.(continued)

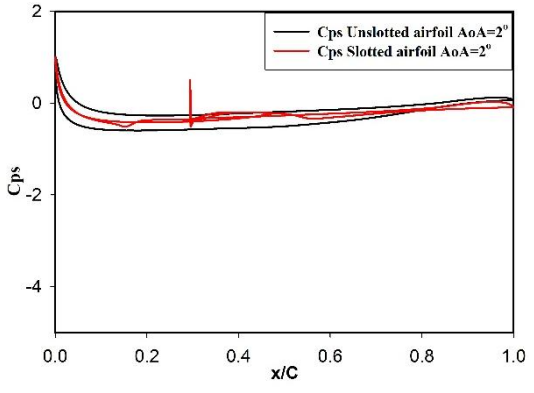

Figure 8 static pressure coefficient for slotted and unslotted airfoil s834 at AoA =2.

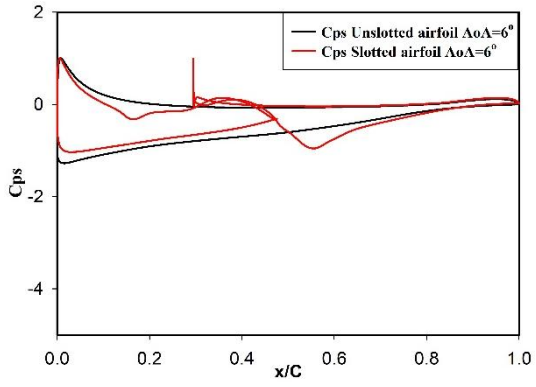

Figure 9 static pressure coefficient for slotted and unslotted airfoil s834 at AoA =6.

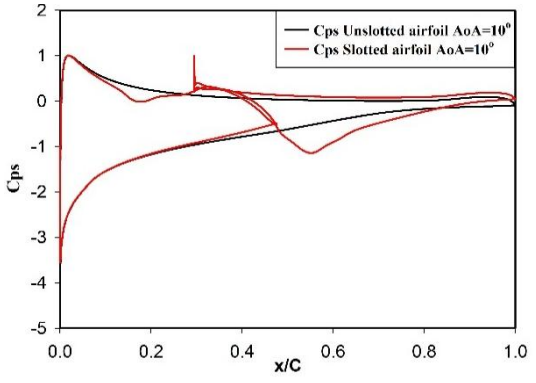

Figure 10 static pressure coefficient for slotted and unslotted airfoil s834 at AoA =10.

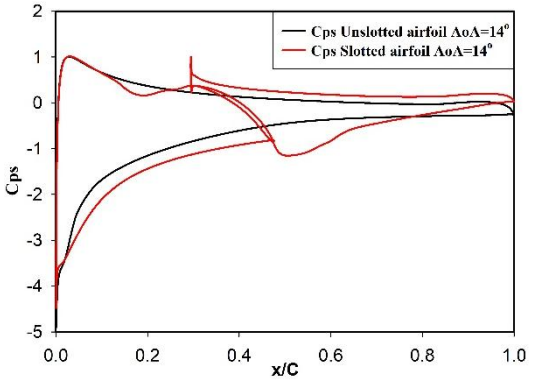

Figure 11 static pressure coefficient for slotted and unslotted airfoil s834 at AoA =14.

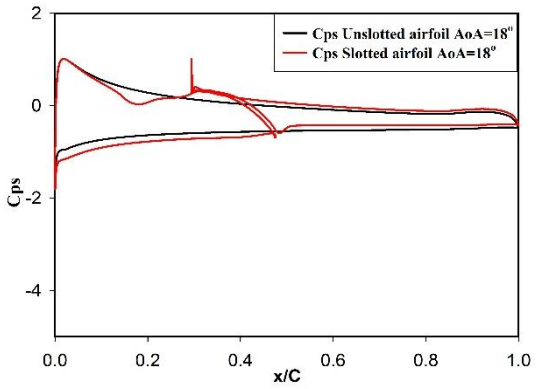

Figure 12 static pressure coefficient for slotted and unslotted airfoil s834 at AoA =18.

4. Conclusion

In this numerical study, the overall performance of the S834 airfoil was numerically analyzed at Reynolds numbers of 0.85 x 105 to assess the effect of a slot on the aerodynamic characteristics. The unsteady numerical simulations were conducted at wind speed of 6 m/s. The excavation of a slot led to a notable enhancement in the performance of the original airfoil. Although the performance of the slotted airfoil was lower than that of the original airfoil at low angles of attack (2° to 8°), it exhibited substantial performance enhancements at higher angles of attack (10° to 16°). The velocity contours and static pressure coefficient revealed notable changes in vortex generation, indicating that the slotted airfoil could contribute to more efficient wind energy utilization and support global sustainability efforts.

References

[1] A. M. Rayhan, M. S. Hossain, R. H. Mim, and M. Ali, "Computational and experimental study on the aerodynamic performance of NACA 4412 airfoil with slot and groove," *Heliyon*, vol. 10, no. 11, p. e31595, 2024, doi: 10.1016/j.heliyon.2024.e31595.

[2] M. E. Hasan, A. Eltayesh, M. I. Awaad, and H. M. El-Batsh, "Experimental Examination for the Electric Power Generation of a Commercial Small-scale Wind Turbine with Modified Aerodynamic Design," *Alexandria Eng. J.*, 2022, doi: 10.1016/j.aej.2022.08.040.

[3] S. D. Skaltsogiannis, E. C. Douvi, D. C. Douvi, and D. P. Margaris, "Simulation of the Flow over NREL's S834 Airfoil at two different Reynolds numbers," *Int. J. New Technol. Res.*, vol. 7, no. 5, 2021, doi: 10.31871/ijntr.7.5.21.

[4] A. Abbaskhah, H. Sedighi, P. Akbarzadeh, and A. Salavatipour, "Optimization of horizontal axis wind turbine performance with the dimpled blades by using CNN and MLP models," *Ocean Eng.*, vol. 276, no. November 2022, p. 114185, 2023, doi: 10.1016/j.oceaneng.2023.114185.

[5] H. Akbıyık, H. Yavuz, and Y. E. Akansu, "Comparison of the Linear and Spanwise-Segmented DBD Plasma Actuators on Flow Control Around a NACA0015 Airfoil," vol. 45, no. 11, pp. 2913–2921, 2017.

[6] T. Yin, G. Pavesi, J. Pei, and S. Yuan, "Numerical investigation on the inhibition mechanisms of unsteady cavitating flow around stepped hydrofoils," *Ocean Eng.*, vol. 265, no. August, p. 112540, 2022, doi: 10.1016/j.oceaneng.2022.112540.